A Compact Millimeter-Wave CMOS Bandpass Filter Using a Dual-Mode Ring Resonator

Sha Luo
Deparment of Electrical and Computer Engineering,
National University of Singapore,
Singapore
eleluos@nus.edu.sg

Aaron V. Do
Analog Design Department,
Marvell Asia Pte Ltd,
Singapore
doaaron82@gmail.com

Chirn Chye Boon, Lei Zhu, and Manh Anh Do
School of Electrical and Electronic Engineering,
Nanyang Technological University,
Singapore

***Abstract*— A stub-loaded dual-mode ring resonator is proposed to design a millimeter-wave bandpass filter using 0.18-μm CMOS Technology. By increasing the length of the open-circuited stub at the inner corner of the ring resonator, the even-mode resonant frequency is moved to a lower frequency to separate it from the odd-mode resonant frequency. Therefore, the center frequency of the passband has been shifted to a lower frequency to achieve a reduced-size filter design. At the same time, an additional transmission zero is brought in at the upper stopband that can be adjusted by the length of the stub as well. Finally, a 60 GHz bandpass filter is fabricated and characterized. The filter has achieved an ultra-compact size of 0.092 x 0.56 mm^2. The measured results show good passband performance with two visible transmission poles and three transmission zeros thereby verifying the design principle.**

Index Terms — stub-loaded, dual-mode, ring resonator, millimeter-wave, bandpass filter.

I. INTRODUCTION

Recently, design of millimeter-wave CMOS-based filters has become very popular. Several millimeter-wave bandpass filters have been explored in 0.18-μm CMOS Technology using thin film microstrip (TFMS) structures [1]-[5]. By using TFMS structures, conventional microstrip theory is still appropriate to analyze the design structures [6], [7]. In [1], two millimeter-wave bandpass filters were designed using simple sinuous-shaped TFMS lines. The measured insertion losses are around 3.7 dB for the 60 GHz filter and 2.7 dB for the 65 GHz filter. However, the fractional bandwidths for both filters are more than 50%, which is too wide for wireless personal area network (WPAN). Two second-order classical Chebyshev filters using parallel-coupled lines were designed to operate at 60 and 77 GHz, respectively, which both have 10% 3-dB fractional bandwidths in [2]. The two filters suffer from high insertion loss, which is 9.3 dB in both passbands. Dual-mode ring resonators have been successfully implemented in millimeter-wave narrow-band bandpass filter designs with low insertion loss, high filtering selectivity and compact size [3]-[5]. In [3], the ring filter was measured to have its center frequency at 64 GHz and a minimum in-band insertion loss of 4.9 dB. Its 3-dB fractional bandwidth is about 18.75%. The chip size is 1.148 x 1.49 mm^2. The ring filter reported in [4] operates at 70 GHz with a minimum in-band insertion loss of 3.6 dB. Its 3-dB fractional bandwith is around 25.71%. By folding the ring structure, the chip size is reduced to 0.65 x 0.67 mm^2. However, in both designs, additional matching networks with high impedance lines and pads were included, which enlarged the overall size and are also not practical when integrating with other devices on chip. Recently, a stepped-impedance dual-mode ring resonator was used to design a bandpass filter [5]. The stepped-impedance structure was formed using a pedestal, which was constructed from multiple vertically stacked finite metal planes connected to the ground plane by via holes. The designed filter achieves a passband with return loss better than 16 dB from 59 to 71 GHz. The minimum in-band insertion loss was measured to be 3.1 dB. The filter has a compact chip area of 0.30 x 0.24 mm^2. For all the filters reported in [3]-[5], one transmission zero appears at the each side of the desired passband.

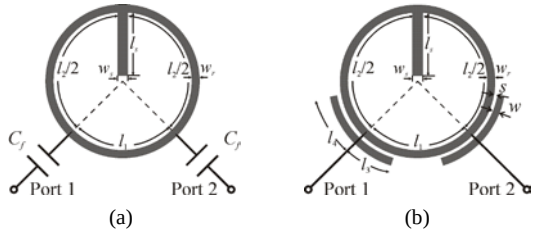

Fig. 1. Schematic of the proposed ring resonator with two distinct excitation structures. (a) By lumped capacitors. (b) By parallel-coupled lines

In this paper, a stub loaded dual-mode ring resonator is proposed to design a 60 GHz narrow-band bandpass filter using a TFMS structure in 0.18 μm CMOS technology. Besides the transmission zero at the each side of the desired passband, the main novelty in

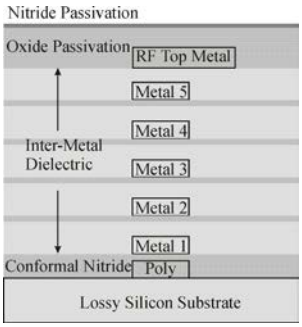

Fig. 2. Layer configuration of the TFMS structure in 0.18 μm CMOS

this design is to bring a third transmission zero at the upper stopband of the filter and at the same time achieve an even more compact size by loading an open-circuited stub at the inner corner of the ring resonator. Finally, a prototype filter is designed and fabricated to verify design theory.

II. Principle of the Proposed Ring Resonator

The proposed dual-mode ring resonators with lumped capacitors (C_f) and parallel-coupled lines at the two excited ports are shown in Fig. 1(a) and (b), respectively. w_r is the width, and l_1 and l_2 are the lengths of the two paths of the ring. The open-circuited stub is loaded at the inner corner of the ring resonator with a width of w_s and a length of l_s. The two pairs of parallel-coupled lines have a width of w and a spacing of s. They are coupled to the ring resonator with lengths of l_3 and l_4, respectively. The layer configuration of a 0.18 μm CMOS technology with six-metal interconnects on a silicon substrate is shown in Fig. 2. The bottom metal layer (Metal 1) is used as a ground plane to minimize the electric field leaking into the silicon region; the top metal layer is used as a conductor plane to keep a maximum distance from the ground plane for high quality factor.

The equivalent circuit model of the ring resonator in Fig. 1(a) is developed as displayed in Fig. 3(a). Its even- and odd-mode circuits are illustrated in Fig. 3(b) and (c), respectively. Z_r and Z_s represent the characteristic impedances of the ring resonator and the open-circuit stub. θ_1 and θ_2 are the electrical lengths of the two paths in the ring; θ_s is the electrical length of the stub. The intrinsic even- and odd-mode resonant frequencies can be derived as algebraic equations as follows, respectively:

$$Z_r \cot\left(\frac{\theta_1+\theta_2}{2}\right) + 2Z_s \cot\theta_s = 0 \quad (1)$$

$$Z_r \tan\left(\frac{\theta_1+\theta_2}{2}\right) = 0\,. \quad (2)$$

From (1) and (2), we observe that the emergence of the stub only influences the even-mode resonant frequency. By increasing the length of the stub, the fundamental even- and odd-mode resonant frequencies can be separated and make up the desired passband. As demonstrated in Fig. 3(d), the passband is stimulated with one or two poles when l_s increases from 200 to 400 μm, and the center

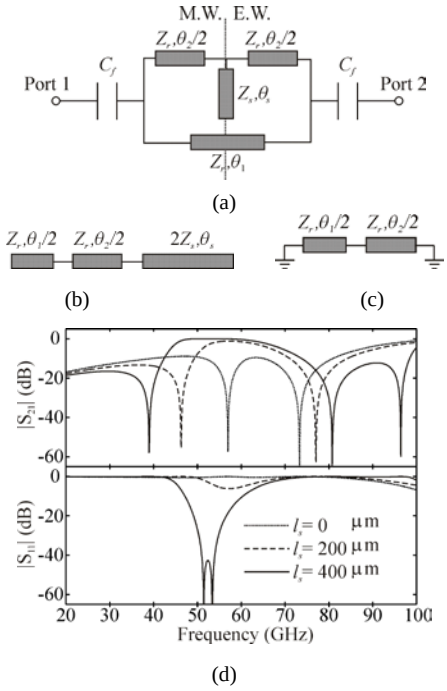

Fig. 3. Proposed ring resonator in Fig. 1(a). (a) The whole equivalent circuit with perfectly M.W. and E. W. at the diagonal line. (b) Even-mode circuit. (c) Odd-mode circuit. (d) Frequency responses of S_{21}-magnitudes for various stub lengths (l_s). (C_f=0.05 pf, w_r= w_s =1.5 μm, l_1=408 μm, and l_2=1880 μm)

frequency of the passband moves to a lower frequency. Meanwhile, two transmission zeros are observed at both sides of the passband. Moreover, there is one more transmission zero appearing at 96 GHz when the stub length is 400 μm.

The equivalent circuit of the proposed ring resonator in Fig. 1(b) is shown in Fig. 4(a). θ_3 and θ_4 are the lower and upper coupling sections, respectively. $Z_c = -2jZ_{0e}Z_{0o} / [(Z_{0e}+Z_{0o}) \tan(\theta_3+\theta_4)]$, $N = (Z_{0e}+Z_{0o}) / (Z_{0e}-Z_{0o})$ and $Z = (Z_{0e}+Z_{0o})/2$, where Z_{0e} and Z_{0o} represent the even- and odd- mode characteristic impedances of the parallel-coupled lines, respectively. Fig. 4(b) shows the influences of the open-circuited stub on the transmission zeros and poles. For l_s = 400 μm, the third transmission zero appears at 97 GHz. As l_s increases from 420 to 440 μm, this zero moves from 94 to 91 GHz. With increasing stub length, only the even-mode resonant frequency moves to a lower frequency and the first two transmission zeros slightly shift away from the passband. The open-circuited stub brings in another transmission zero, which can be properly positioned to further improve the rejection in the upper stopband.

III. Results and Discussion

Based on the above analysis, a dual-mode bandpass filter was designed on a 0.18 μm CMOS multi-layered structure. The folding technique was implemented to further reduce the overall size of the filter. Fig. 5(a) shows the physical layout of the designed filter. The microphotograph of the chip is shown in Fig. 5(b). To our

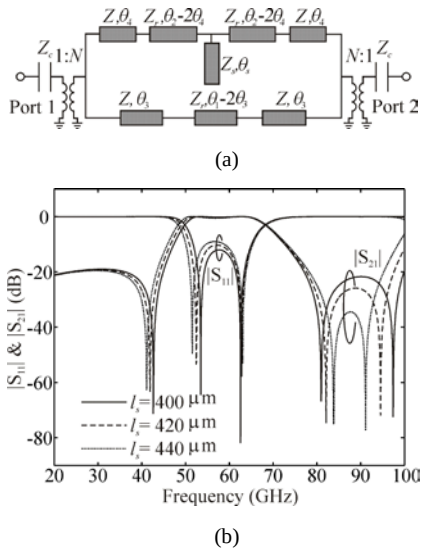

Fig. 4. Proposed ring resonator in Fig. 1 (b). (a) Equivalent circuit model. (b) Frequency responses of *S*-magnitudes under various stub lengths (l_s) (w_r= w_s =1.5 μm, l_1=408 μm, l_2=1880 μm, s =2.99 μm, w =1.5 μm, l_3=164 μm, and l_4=396 μm).

best knowledge, this filter is the smallest reported CMOS 60 GHz filter, which occupies an area of 0.092x 0.56 mm^2. The filter was characterized on wafer after calibration with respect to the reference planes of the RF probes. The measurement data was further de-embedded to eliminate pad and feeding line influence, and other EM parasitic effects [8].

The simulated results from both circuit model and full-wave EM simulator [9], and the measured results after de-embedding are plotted together in Fig. 5(c). A reasonably good agreement between the three sets of results in the frequency range from 20 to 100 GHz is observed. The measured center frequency is at 62 GHz with a minimum in-band insertion loss of 4.9 dB. This insertion loss is mainly contributed by the conductor loss and the dielectric loss. The 3-dB passband is around 24 % with a frequency range from 55 to 70 GHz. The measured return loss is better than 7 dB in the passband. The three transmission zeros occur at 44, 77 and 97 GHz as expected. The rejection in the lower stopband is higher than 25 dB from DC to 47 GHz; the rejection in the upper stopband is greater than 21 dB from 76 to 100 GHz.

IV. Conclusion

In this work, a dual-mode stub-loaded ring resonator has been successfully implemented to design a 60 GHz bandpass filter using 0.18 μm CMOS technology. Conventional microstrip theory has been applied to develop the equivalent circuit model of the proposed ring resonator and to predict the filter performances. Finally, a 60 GHz bandpass filter has been fabricated and measured. The filter has achieved an ultra-compact size of 0.092 x 0.56 mm^2. Predicted results were verified experimentally, showing two transmission poles in the desired passband and three zeros in stopband.

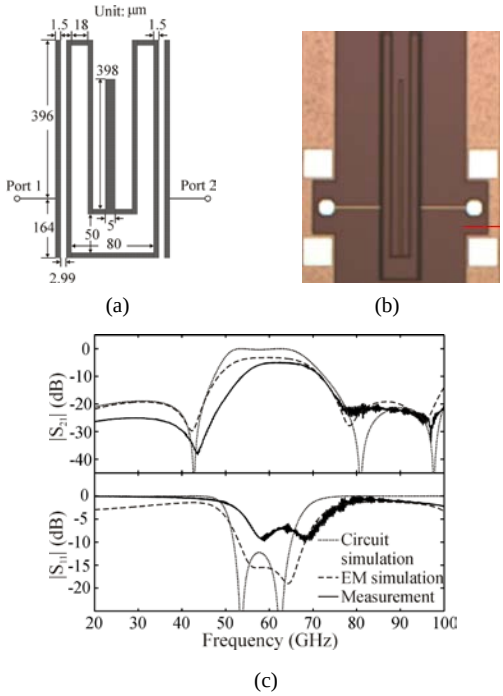

Fig. 5. Fabricated filter. (a) Physical layout. (b) Microphotograph. (c) Simulated and measured *S*-magnitudes

[1] S. Sun, J. Shi, L. Zhu, S. C. Rustagi, and K. Mouthaan, "Millimeter-wave bandpass filters by standard 0.18-μm CMOS technology," *IEEE Electron Device Lett.*, vol. 28, No. 3, pp.220-222, Mar. 2007.

[2] L. Nan, K. Mouthaan, Y. -Z. Xiong, J. Shi, S. C. Rustagi, and B. -L. Ooi, "Design of 60- and 77-GHz narrow-bandpass filters in CMOS technology," *IEEE Trans. Circuit Syst. II: Express Brief*, vol. 55, no. 8, pp. 738–742, Aug. 2008.

[3] C. -Y. Hsu, C. -Y. Chen and H. -R. Chuang, "A 60 GHz millimeter-wave bandpass filter using 0.18-μm CMOS technology," *IEEE Electron Device Lett.*, vol.29, no.3, pp.246-248, Mar. 2008.

[4] C. -Y. Hsu, C. -Y. Chen and H. -R. Chuang, "70 GHz folded loop dual-mode bandpass filter fabricated using 0.18 μm standard CMOS technology," *IEEE Microw. Wireless Compon. Lett.*, vol. 18, no. 9, pp. 587-589, Sep. 2008.

[5] S. -C. Chang, Y. -M. Chen, S. -F. Chang, Y. -H. Jeng, C. -L. Wei, C. -H. Huang, and C. -P. Jeng, "Compact millimeter-wave CMOS bandpass filters using grounded pedestal stepped-impedance technique," *IEEE Trans. Microw. Tehory Tech.*, vol. 58, no. 12, pp. 3850-3858, Dec. 2010.

[6] G. E. Ponchak and A. N. Downey, "Characterization of thin film microstrip lines on polymide," *IEEE Trans. Compon., Packag., Manuf. Technol. B*, vol. 21, no. 2, pp. 171-176, May 1998.

[7] G. Prigent, E. Rius, F. L. Pennec, S. L. Magure, C. Quendo, G. Six, and H. Happy, "Design of narrow DBR planar filters in Si-BCB technology for millimeter-wave applications," ," *IEEE Trans. Microw. Tehory Tech.*, vol. 52, no. 3, pp. 1045-1050, Mar. 2004.

[8] E. P. Vandamme, D. M. M. -P, and C. V. Dinther, "Improved three-step de-embedding method to accurately account for the influence of pad parasitics in silicon on-wafer RF test-structures," *IEEE Electron Device Lett.*, vol.48, no.4, pp.737-742, Apr. 2001.

[9] *CST Microwave Studio, Computer Simulation Technology*, Wellesley Hills, MA 02481.